2001 IEEE/ASME International Conference on
Advanced Intelligent Mechatronics Proceedings
8—12 July 2001 • Como, Italy

Rest-to-Rest Motion of a One-link Flexible Arm

Alessandro De Luca Giandomenico Di Giovanni

Università degli Studi di Roma "La Sapienza"
Dipartimento di Informatica e Sistemistica
Via Eudossiana 18, 00184 Roma, Italy
deluca@dis.uniroma1.it
http://labrob.ing.uniroma1.it

Abstract— **We present a solution to the problem of finding the torque command that provides rest-to-rest motion in a given time for a one-link flexible arm. The basic idea is to design an auxiliary output such that the associated transfer function has no zeros. Planning a smooth interpolating trajectory for this output imposes a unique rest-to-rest motion to the whole arm, with automatically bounded link deformation. The nominal torque is then obtained by inverse dynamics computation in the time domain. The method is presented for a linear model based on the Euler-Bernoulli beam description of the flexible link with dynamic boundary conditions. This approach lends itself to nonlinear extensions and feedback solutions.**

I. Introduction

The basic problem of moving a manipulator from one equilibrium configuration to another in a prescribed time becomes critical in the presence of link flexibility, introduced by a long reach and slender/lightweight construction of the arm [1]. The gross motion induces residual oscillations at the nominal final time, extending thus the time horizon before the arm can be considered at rest. Indeed, link vibrations may eventually vanish due to the damping injected by a feedback controller [2] and/or inherent in the structure [3]. This, however, reduces the practical performance of the robotic task when fast and precise positioning is needed.

Several approaches have been proposed for the rest-to-rest motion problem of flexible arms. Two basic model-based methods are input shaping [4], [5], [6] and inverse dynamics trajectory design [7], [8], [9]. Given a desired reconfiguration task, input shaping consists in convolving the reference command (a step input) with impulses, suitably located in time, that 'kill' the modal frequencies of the flexible arm. The method is straightforward for one or few flexible modes [4], but more complex when increasing the number of considered modes, or for achieving robustness [6]. On the other hand, one can design a smooth interpolating trajectory for the end-effector of a flexible arm and then use stable input-output inversion for computing the rest-to-rest torque command with bounded link deformations during motion. This approach was pioneered by Bayo in the frequency domain [7] and revisited later in the time domain in [9]. However, there are two drawbacks for the problem at hand: first, the computed nominal torques are non-causal, extending in time both before the start and after the completion of the desired end-effector trajectory; second, the practical accuracy in the vanishing of link deformations is limited by the finite window in time (or in frequency) used in the implementation. Another possible technique for residual vibration suppression uses optimal control theory [10] but needs to resort in general to numerical solutions. Finally, in [11], [12] a different approach has been proposed for a one-link flexible arm. In [11], a combination of sinusoidal components is used to build up a rest-to-rest joint trajectory, from which the nominal torque command is obtained via inversion. In [12], the rest-to-rest motion involves planning a suitable end-effector trajectory so as to cancel the effect of non-minimum phase zeros in the (inverse of the) associated torque-tip angle transfer function. Both methods are intrinsically linear and require the solution of linear algebraic systems that are ill-conditioned for increasing number of flexible modes.

In this paper, we design a system output with maximum relative degree, i.e., such that no zeros appear in the trasfer function from the input torque to the defined output. The rest-to-rest motion problem is then solved by fitting to this output a smooth polynomial interpolating the start and final rest configurations. Building on the preliminary result of [13], it is shown that such a design output, as well as the associated nominal rest-to-rest torque, can be computed in closed form for a general linear model of a one-link flexible arm (including also modal damping). Our method applies also to more general state-to-state transfers, e.g., from an initial state with link deformation and possibly nonzero velocity to a desired final equilibrium state with zero deformation. In addition, generalization to nonlinear settings is in principle feasible since the computations rely only on time and state concepts. Numerical results are included showing the effectiveness of the method. Finally, we discuss how the obtained nominal feedforward torque and state evolution can be used within a stabilizing feedback controller.

II. Dynamic model of a flexible arm

Consider an arm having a single rotating flexible link of length ℓ and uniform linear mass density ρ, and moving on the horizontal plane. We assume small deformations limited to the plane of motion. The arm is driven by an electrical actuator at the base, with inertia J_0 and torque $\tau(t)$, and carries a tip payload of mass M_p and inertia J_p. We model the flexible link as an Euler-Bernoulli beam with Young modulus E and inertia of the cross section I. Let $\theta(t)$ be the angle of a line pointing at the instantaneous

0-7803-6736-7/01/$10.00 © 2001 IEEE

center of mass of the link w.r.t. an inertial frame (pinned angle). The transversal bending deformation at a point $x \in [0, \ell]$ along the link is described by $w(x,t)$.

From Hamilton's principle, the flexible arm satisfies the following equations of motion [14], [15]

$$\begin{aligned} EIw''''(x,t) + \rho\Big(\ddot{w}(x,t) + x\ddot{\theta}(t)\Big) &= 0 \\ \tau(t) - J\ddot{\theta}(t) &= 0, \end{aligned}$$

where $J = J_0 + (\rho\ell^3)/3 + J_p + M_p\ell^2$ is the total inertia of the arm w.r.t. the joint axis, with associated dynamic boundary conditions given by

$$\begin{aligned} w(0,t) &= 0 \\ EIw''(0,t) &= J_0\Big(\ddot{\theta}(t) + \ddot{w}'(0,t)\Big) - \tau(t) \\ EIw''(\ell,t) &= -J_p\Big(\ddot{\theta}(t) + \ddot{w}'(\ell,t)\Big) \\ EIw'''(\ell,t) &= M_p\Big(\ell\ddot{\theta}(t) + \ddot{w}(\ell,t)\Big), \end{aligned}$$

denoting by a prime the spatial derivative w.r.t. x.

By separation in space and time, assuming a finite number n_e of deformation mode shapes $\phi_i(x)$ with associated deformation coordinates $\delta_i(t)$,

$$w(x,t) = \sum_{i=1}^{n_e} \phi_i(x)\delta_i(t),$$

the free evolution ($\tau = 0$) of the system is characterized by the solutions to

$$\begin{aligned} EI\phi_i^{IV}(x) - \rho\omega_i^2\phi_i(x) &= 0 \\ \ddot{\delta}_i(t) + \omega_i^2\delta_i(t) &= 0, \end{aligned}$$

being ω_i the eigenfrequencies of the flexible arm, with spatial boundary conditions

$$\begin{aligned} \phi_i(0) &= 0 \\ EI\phi_i''(0) + \omega_i^2 J_0\,\phi_i'(0) &= 0 \\ EI\phi_i''(\ell) - \omega_i^2 J_p\,\phi_i'(\ell) &= 0 \\ EI\phi_i'''(\ell) + \omega_i^2 M_p\,\phi_i(\ell) &= 0, \end{aligned}$$

for $i = 1, \ldots, n_e$. The general solutions are in the form

$$\begin{aligned} \phi_i(x) &= A_i\sin(\beta_i x) + B_i\cos(\beta_i x) \\ &\quad + C_i\sinh(\beta_i x) + D_i\cosh(\beta_i x), \end{aligned} \tag{1}$$

where $\beta_i^4 = \rho\omega_i^2/EI$ and $\beta_1, \ldots, \beta_{n_e}$ are the first n_e roots of the following characteristic equation

$$\begin{aligned} &(c\,sh - s\,ch) - \frac{2M_p}{\rho}\beta_i\,s\,sh - \frac{2J_p}{\rho}\beta_i^3\,c\,ch \\ &-\frac{J_0}{\rho}\beta_i^3(1 + c\,ch) - \frac{M_p}{\rho^2}\beta_i^4(J_0 + J_p)(c\,sh - s\,ch) \\ &+\frac{J_0 J_p}{\rho^2}\beta_i^6(c\,sh + s\,ch) - \frac{J_0 J_p M_p}{\rho^3}\beta_i^7(1 - c\,ch) = 0, \end{aligned}$$

with $s = \sin(\beta_i\ell)$, $c = \cos(\beta_i\ell)$, $sh = \sinh(\beta_i\ell)$, and $ch = \cosh(\beta_i\ell)$. Using the orthonormality conditions on the mode shapes, the Euler-Lagrange equations for the $N = n_e + 1$ generalized coordinates $q = (\theta, \delta) = (\theta, \delta_1, \ldots, \delta_{n_e})$ yield

$$J\ddot{\theta} = \tau \tag{2}$$

$$\ddot{\delta}_i + \omega_i^2\delta_i = \phi_i'(0)\tau, \qquad 1, \ldots, n_e. \tag{3}$$

It is easy to check that the linear dynamic model (2–3) is controllable.

Note finally that the transfer function from τ to the clamped joint output

$$\theta_c = \theta + \sum_{i=1}^{n_e} \phi_i'(0)\delta_i \tag{4}$$

is minimum phase (zeros in the left hand side of the complex plane), while the transfer function from τ to the tip output

$$y_t = \theta + \sum_{i=1}^{n_e} \frac{\phi_i(\ell)}{\ell}\,\delta_i \tag{5}$$

is non-minimum phase. Other relevant output functions for a flexible arm have been considered in the literature (see [16] and [17]), but all the associated transfer functions include stable or unstable zeros.

III. Rest-to-rest motion design

Consider a desired rest-to-rest motion task for the one-link flexible arm modeled by eqs. (2–3). The arm should be moved from an initial undeformed configuration $q_i = (\theta_i, 0)$ at $t_i = 0$ to a final undeformed configuration $q_f = (\theta_f, 0)$ at time $t_f = T$, with $\dot{q}(0) = \dot{q}(T) = 0$.

We can solve this problem by designing an output function y such that the associated transfer function will have no zeros. This design output has the form

$$y = \theta + \sum_{i=1}^{n_e} c_i\delta_i = \theta + c^T\delta, \tag{6}$$

with the coefficients c_i ($i = 1, \ldots, n_e$) to be determined by imposing the condition that the output (6) has maximum relative degree (equal to the state space dimension $2(n_e+1)$ of the flexible arm), i.e., y and its first $2n_e + 1$ derivatives are independent from the input τ.

Due to the second order structure of eqs. (2–3), the torque may appear only in the first n_e even derivatives. From

$$\ddot{y} = \Big(\frac{1}{J} + \sum_{i=1}^{n_e} c_i\phi_i'(0)\Big)\tau - \sum_{i=1}^{n_e} c_i\omega_i^2\delta_i,$$

we set $\sum c_i\phi_i'(0) = -1/J$. Next,

$$y^{[4]} = \frac{d^4y}{dt^4} = -\sum_{i=1}^{n_e} c_i\omega_i^2\phi_i'(0)\,\tau + \sum_{i=1}^{n_e} c_i\omega_i^4\delta_i$$

from which $\sum c_i\omega_i^2\phi_i'(0) = 0$. Proceeding further until the $(2n_e+1)$-th output derivative, we finally obtain the following linear system of equations, which can be always solved in the (unique) unknown vector of coefficients c,

$$V\,\mathrm{diag}\{\phi_1'(0), \ldots, \phi_{n_e}'(0)\}\,c = b, \tag{7}$$

with $b = [-1/J\ 0\ \dots\ 0]^T$ and Vandermonde matrix

$$V = \begin{bmatrix} 1 & 1 & \dots & 1 \\ \omega_1^2 & \omega_2^2 & \dots & \omega_{n_e}^2 \\ \omega_1^4 & \omega_2^4 & \dots & \omega_{n_e}^4 \\ & \dots & & \\ \omega_1^{2(n_e-1)} & \omega_2^{2(n_e-1)} & \dots & \omega_{n_e}^{2(n_e-1)} \end{bmatrix},$$

being nonsingular since $\omega_i \neq \omega_j$, for $i \neq j$.

The numerical solution of eq. (7) becomes, however, ill-conditioned for large n_e (similarly to the methods in [11], [12]). On the other hand, the first column of the inverse of the V matrix can be given an explicit expression in terms of the determinant a lower order Vandermonde matrix. Performing computations leads then to a closed form solution for the coefficients c_i:

$$c_i = -\frac{1}{J\phi_i'(0)} \prod_{\substack{j=1 \\ j\neq i}}^{n_e} \frac{\omega_j^2}{\omega_j^2 - \omega_i^2}, \qquad i = 1, \dots, n_e. \tag{8}$$

We note that these coefficients can be also recovered by a Laplace argument, by transforming eqs. (2), (3), and (6), computing the transfer function $y(s)/\tau(s)$, and finally imposing a constant numerator, i.e.,

$$\frac{y(s)}{\tau(s)} = \frac{1}{Js^2} + \sum_{i=1}^{n_e} \frac{c_i\phi_i'(0)}{s^2+\omega_i^2} = \frac{K}{s^2\prod_{i=1}^{n_e}(s^2+\omega_i^2)}. \tag{9}$$

Using partial fractions expansion leads to the values (8) and to $K = \prod_{i=1}^{n_e}\omega_i^2/J$.

The design output (6) is used, together with its derivatives up to the order $2n_e+1$, as a new state representation of the system, through the following invertible transformation

$$\begin{bmatrix} y \\ \ddot{y} \\ \vdots \\ y^{[2n_e]} \end{bmatrix} = Q \begin{bmatrix} \theta \\ \delta_1 \\ \vdots \\ \delta_{n_e} \end{bmatrix}, \qquad \begin{bmatrix} \dot{y} \\ y^{[3]} \\ \vdots \\ y^{[2n_e+1]} \end{bmatrix} = Q \begin{bmatrix} \dot{\theta} \\ \dot{\delta}_1 \\ \vdots \\ \dot{\delta}_{n_e} \end{bmatrix}, \tag{10}$$

where

$$Q = \begin{bmatrix} 1 & c_1 & \dots & c_{n_e} \\ 0 & -c_1\omega_1^2 & \dots & -c_{n_e}\omega_{n_e}^2 \\ & & \dots & \\ 0 & (-1)^{n_e}c_1\omega_1^{2n_e} & \dots & (-1)^{n_e}c_{n_e}\omega_{n_e}^{2n_e} \end{bmatrix}. \tag{11}$$

The rest-to-rest motion problem can then be solved by defining an interpolating trajectory $y = y_d(t)$, with appropriate boundary conditions at time $t_i = 0$ and $t_f = T$. From the structure of eqs. (10–11), it is enough to simply put $y_d(0) = \theta_i$, $y_d(T) = \theta_f$, with all derivatives up to the $(2n_e+1)$-th equal zero at the initial and final time. For satisfying these boundary conditions, a polynomial of degree $4n_e + 3$ will be sufficient.

For a generic state-to-state transfer, one can still use the same approach by mapping any desired values of the state $(\theta, \delta, \dot{\theta}, \dot{\delta})$ at the initial and final time into boundary conditions for the interpolating polynomial $y_d(t)$ and its derivatives.

The nominal torque for a state-to-state transfer in time T is finally computed by inversion of the highest order output derivative expression, imposing $y^{[2(n_e+1)]} = y_d^{[2(n_e+1)]}$:

$$\tau_d(t) = \frac{y_d^{[2(n_e+1)]}(t) - (-1)^{n_e+1}\sum_{i=1}^{n_e} c_i\omega_i^{2(n_e+1)}\delta_i(t)}{(-1)^{n_e}\sum_{i=1}^{n_e} c_i\omega_i^{2n_e}\phi_i'(0)}, \tag{12}$$

with $t \in [0, T]$. In eq. (12), the values of δ are obtained algebraically by inverting the linear system of equations (10) having set $y \equiv y_d(t)$. The transformation matrix Q can be manipulated so as to let again the Vandermonde matrix V appear.

In the specific case of rest-to-rest motion, a closed form expression of the nominal torque can obtained without the need of computing neither the coefficients c_i nor the inverse of Q. In fact, setting $y = y_d$ in eq. (9), we obtain in the Laplace domain

$$\tau_d(s) = \frac{J}{\prod_{i=1}^{n_e}\omega_i^2}\left[s^2\prod_{i=1}^{n_e}(s^2+\omega_i^2)\right] y_d(s),$$

and thus in the time domain

$$\tau_d(t) = \frac{J}{\prod_{i=1}^{n_e}\omega_i^2}\left[y_d^{[2(n_e+1)]}(t) + \sum_{i=0}^{n_e-1}\alpha_i y_d^{[2(i+1)]}(t)\right], \tag{13}$$

with coefficients α_i easily obtained by convolution of polynomial coefficients. For example, for $n_e = 3$, we have

$$\alpha_0 = \prod_{i=1}^{3}\omega_i^2, \qquad \alpha_1 = \sum_{i=1}^{3}\frac{\prod_{j=1}^{3}\omega_j^2}{\omega_i^2}, \qquad \alpha_2 = \sum_{i=1}^{3}\omega_i^2.$$

A series of remarks are in order.

- Although computations are simpler when using the eigenfunctions (1) as assumed modes and expressing link deformation in the pinned reference frame (leading to eqs. (2–3)), the same method can be applied to any other linear model and reference frame for the one-link flexible arm, provided that the system is controllable. In fact, the state-space transformation (10) is just an explicit derivation of the controllable canonical form for linear single-input systems.
- Along the same line, the numerical values entering in the model (2–3) (i.e., the total arm inertia J, the eigenfrequencies ω_i, and the spatial tangents $\phi_i'(0)$ at the link base —which act as input gains) may be also the outcome of an experimental identification performed on the flexible arm.
- Inclusion of modal damping can be handled in a similar way. For a dynamic model of the form

$$\begin{aligned} J\ddot{\theta} &= \tau \\ \ddot{\delta}_i + 2\zeta_i\omega_i\dot{\delta}_i + \omega_i^2\delta_i &= \phi_i'(0)\tau, \qquad 1, \dots, n_e, \end{aligned}$$

where $\zeta_i \in (0,1)$ is the damping coefficient of the ith mode, the structure of the design output is modified as

$$y = \theta + \sum_{i=1}^{n_e} c_i \delta_i + \gamma \dot{\theta} + \sum_{i=1}^{n_e} d_i \dot{\delta}_i, \qquad (14)$$

and the $2(n_e+1)$ unknown coefficients are computed as before, by imposing the maximum relative degree to the output (14). Even in this case, a closed form expression can be derived for γ, the c_i's, and d_i's, reasoning in terms of partial fractions expansion and residuals —as with eq. (9).

• Let $c_i^{(k)}$ $(i = 1, \ldots, k)$ be the set of output coefficients obtained when assuming k modes in the dynamic modeling. It is interesting to analyze the behavior of the numerical values of these coefficients when increasing the number of assumed modes. It is easy to see that

$$c_i^{(k+1)} = c_i^{(k)} \frac{\omega_{k+1}^2}{\omega_{k+1}^2 - \omega_i^2}, \qquad i = 1, \ldots, k,$$

being the eigenfrequencies ω_i and eigenvectors $\phi_i(x)$ independent from the number of modes considered in the expansion. Therefore, since the sequence $\{\omega_i\}$ is fast increasing, the lowest order coefficients (say, for i up to $k/2$) converge rapidly to a constant value for increasing k.

• By choosing an interpolating polynomial of order $4n_e+5$, one can impose also $y_d^{[2(n_e+1)]} = 0$ at the initial and final time, so that the nominal torque profile given by eq. (12) starts and ends at zero. Higher order polynomials with symmetric zero boundary conditions for the derivatives would achieve further smoothness of the nominal torque.

• A common criticism to the use of smooth high-order polynomials as motion trajectories for flexible arms is that too much of the available motion time is wasted in excessively slow starting and arriving phases. Accordingly, larger peak torque values attained only for few instants are required for the same total motion time (see also the numerical results in Sect. IV). The presented method can be modified so as to generate bang-bang or bang-coast-bang type of torque profiles, with smooth interpolating phases near the start and final (and midway) instants. Actuator capabilities are then much better used: with the data used in Sect. IV, we obtained a reduction of 70% (!) of the peak torque for the same motion time T.

IV. Numerical results

We have applied the presented method to a flexible arm with the following data:

$$\begin{aligned} \ell &= 0.7\ \text{m} \\ \rho &= 2.975\ \text{kg/m} \\ EI &= 2.4507\ \text{N m}^2 \\ J_0 &= 1.95 \cdot 10^{-3}\ \text{kg m}^2 \\ M_p &= 0.117\ \text{kg} \\ J_p &= 0. \end{aligned}$$

The first three modal frequencies of the flexible arm are: $f_1 = 4.0524$, $f_2 = 12.3440$, and $f_3 = 22.8727$ (Hz).

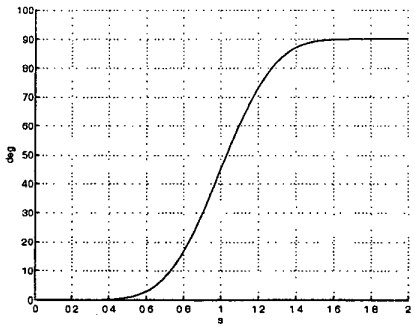

Fig. 1. Interpolating profile for the design output

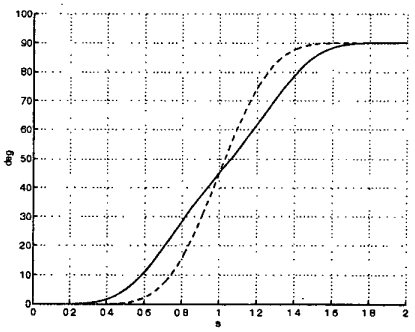

Fig. 2. Evolution of clamped joint angle (—) and tip angle (- -)

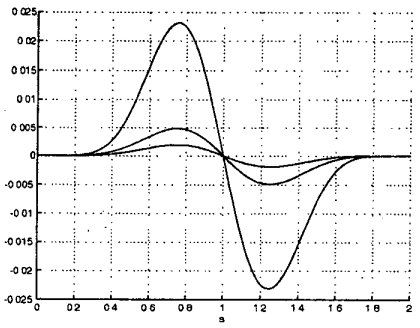

Fig. 3. Evolution of first three flexible modes

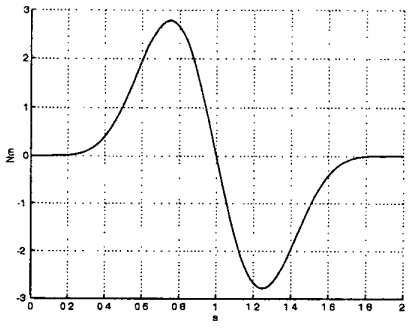

Fig. 4. Rest-to-rest motion torque

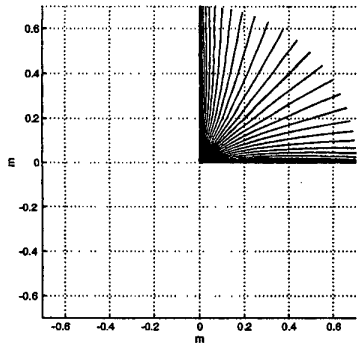

Fig. 5. Stroboscopic view of the flexible arm

Figures 1–5 show the results of a rest-to-rest slew motion of 90° in $T = 2$ s considering $n_e = 3$ modes. The design output trajectory shown in Fig. 1 is a 19th-degree polynomial, chosen so as to guarantee continuity also of the torque derivative. The clamped joint angle given by eq. (4) and the tip angle given by eq. (5) have a symmetric behavior in time (Fig. 2): in the first half of motion, the joint angle leads the output trajectory while the tip angle lags behind; the situation is reversed in the second half. The three deformation variables δ are well within the assumed domain of linearity (Fig. 3). The input torque in Fig. 4 is zero outside the interval $[0, T]$.

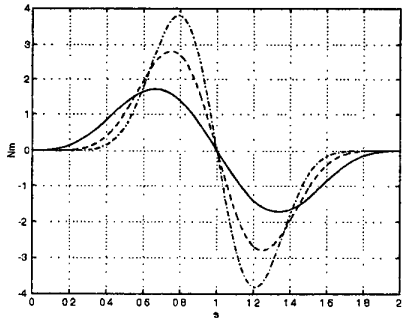

Fig. 6. Rest-to-rest torque: $n_e = 1$ (—), $n_e = 3$ (- -), $n_e = 5$ (- .)

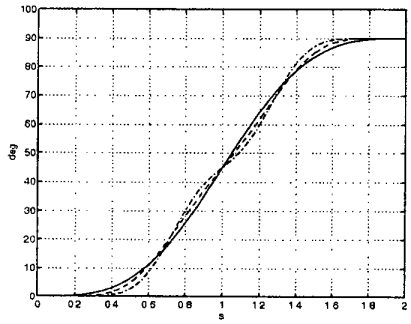

Fig. 7. Clamped joint angle: $n_e = 1$ (—), $n_e = 3$ (- -), $n_e = 5$ (- .)

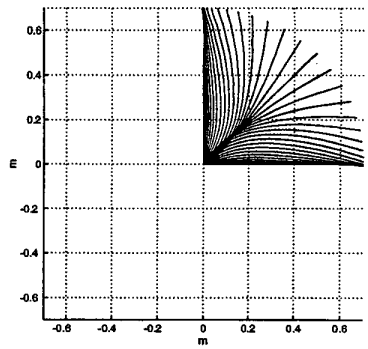

Fig. 8. Stroboscopic view of the flexible arm (faster motion)

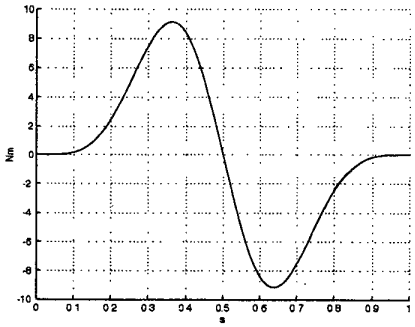

Fig. 9. Rest-to-rest motion torque (faster motion)

In Figs. 6 and 7, we compare the nominal torque and clamped joint angle profiles for increasing number of considered modes. The torque is more concentrated in the middle of the time interval and has an higher peak for larger values of n_e, due to the need of progressively higher order interpolating polynomials for motion planning. The clamped joint angles are quite similar for changing n_e.

Finally, Figs. 8–10 show the results of the same rest-to-rest motion of 90° performed twice as fast with $T = 1$ s. The peak torque for this rest-to-rest motion (Fig. 9) is more than three times larger than before. The maximum angu-

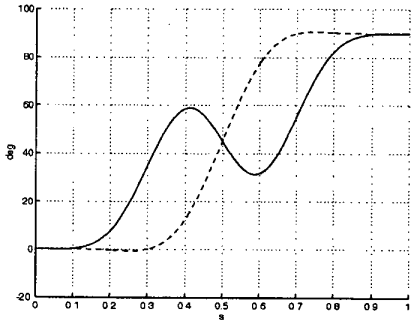

Fig. 10. Evolution of clamped joint angle (—) and tip angle (- -) (faster motion)

lar deflection between the clamped joint angle at the link link and the angle pointing at the arm tip becomes as large as 50°: the assumption of small deformation does not hold anymore and a practical lower bound to the motion duration can be deduced. Similar results have been obtained for $T = 2$ s but payload mass increased by a factor of ten.

V. Feedback control

In the presence of inaccurate information on the actual initial state, small disturbances, or model uncertainties, the use of the nominal feedforward command (12) is not satisfactory. On the other hand, the presented method computes off-line the full state evolution of the flexible arm associated to the desired rest-to-rest reconfiguration. In particular, the reference behavior of the clamped joint output (4) and of its derivative $\dot{\theta}_c$ are obtained from eq. (10) as functions of the desired design output profile $y_d(t)$ and its derivatives. The actual values of these two quantities can be directly measured by an encoder mounted on the actuating motor.

In order to achieve a robust behavior using a simple linear feedback controller, a joint PD scheme with feedforward compensation can be designed as

$$\tau = \tau_d + k_p(\theta_{c,d} - \theta_c) + k_d(\dot{\theta}_{c,d} - \dot{\theta}_c), \qquad (15)$$

where $k_p > 0$, $k_d > 0$, τ_d is given by eq. (12), and $\theta_{c,d}$ and $\dot{\theta}_{c,d}$ are obtained by inverting the state transformation (10) with $y = y_d(t)$ (in particular, the position reference of the joint clamped angle is displayed in Fig. 2).

The controller (15) guarantees exponential stability of the trajectory tracking error. In particular, once the nominal time T is reached, $\theta_{c,d}(t) = \theta_f$ and $\tau_d(t) = \dot{\theta}_{c,d}(t) = 0$ (for $t \geq T$), so that the final regulation is obtained through the stabilizing PD feeback from the partial state $(\theta_c, \dot{\theta}_c)$ [2]. This result holds also for more general multi-input flexible manipulators with nonlinear dynamics [18].

VI. Conclusions

We have presented a new method for computing the nominal torque that achieves rest-to-rest motion (or, more in general, state-to-state transfer) in given time for a one-link flexible arm. It is based on a design output with maximum relative degree (no zeros in the associated transfer function) and on input-output inversion of the system dynamics, which can be both computed in closed form.

Physically, this design output is the angle pointing to a specific location on the arm where there is a crossing (through infinity) from minimum to non-minimum phase zeros in the associated trasfer function, while moving the output from the hub to the tip (see eqs. (4) and (5)). Its use allows to obtain very satisfactory performance with a natural resulting motion of the flexible arm. Preliminary results show also that the method is conveniently insensitive to neglected higher order modes. The nominal state evolution and feedforward command can be used within a joint PD controller, for a simple but effective feedback execution of rest-to-rest motion in the presence of moderate uncertainties in the dynamic parameters (see [19]).

Since the concept of zero dynamics migrates also to a nonlinear setting, the generalization of the method to multi-link flexible arms is feasible and has been considered in an accompanying paper [20].

Acknowledgments

Work supported by MURST under MISTRAL project.

References

[1] W. J. Book, "Modeling, design, and control of flexible manipulator arms: A tutorial review," *29th IEEE Conf. on Decision and Control*, pp. 500–506, 1990.

[2] S. Cetinkunt and W.-L. Yu, "Closed-loop behavior of a feedback-controller of a flexible arm: A comparative study," *Int. J. of Robotics Research*, vol. 10, no. 3; pp. 263–275, 1991.

[3] S. W. Kung and R. Singh, "Vibration analysis of beams with multiple constrained layer damping patches," *J. of Sound and Vibration*, vol. 212, no. 5; pp. 781–805, 1998.

[4] N. C. Singer and W. P. Seering, "Design and comparison of command shaping methods for controlling residual vibration," *1989 IEEE Int. Conf. on Robotics and Automation*, pp. 888–893, 1989.

[5] N. C. Singer and W. P. Seering, "Preshaping command inputs to reduce system vibration," *ASME J. of Dynamic Systems, Measurements, and Control*, vol. 112, pp. 76–82, 1990.

[6] J.M. Hyde and W. P. Seering, "Using input command preshaping to suppress multiple mode vibration," *1991 IEEE Int. Conf. on Robotics and Automation*, pp. 2604–2609, 1991.

[7] E. Bayo, "A finite-element approach to control the end-point motion of a single-link flexible robot," *J. of Robotic Systems*, vol. 4, no. 1, pp. 63–75, 1987.

[8] E. Bayo and B. Paden, "On trajectory generation for flexible robots," *J. of Robotic Systems*, vol. 4, no. 2, pp. 229–235, 1987.

[9] D.-S. Kwon and W. J. Book, "An inverse dynamic method yielding flexible manipulator state trajectories," *1990 American Control Conf.*, pp. 186–193, 1990.

[10] S. P. Bhat and D. K. Miu, "Precise point-to-point positioning control of flexible structures," *ASME J. of Dynamic Systems, Measurements, and Control*, vol. 112, pp. 667–674, 1990.

[11] H. Yang, H. Krishnan, and M. H. Ang Jr., "A simple rest-to-rest control command for a flexible link robot," *1997 IEEE Int. Conf. on Robotics and Automation*, pp. 3312–3317, 1997.

[12] M. Benosman and G. Le Vey, "End-effector motion planning for one-link flexible robot," *6th IFAC Symp. on Robot Control*, pp. 561–566, 2000.

[13] A. De Luca, "Feedforward/feedback laws for the control of flexible robots," *2000 IEEE Int. Conf. on Robotics and Automation*, pp. 233–240, 2000.

[14] E. Barbieri and Ü. Özgüner, "Unconstrained and constrained mode expansions for a flexible slewing link," *ASME J. of Dynamic Systems, Measurement, and Control*, vol. 110, pp. 416–421, 1988.

[15] F. Bellezza, L. Lanari, and G. Ulivi, "Exact modeling of the slewing flexible link," *1990 IEEE Int. Conf. on Robotics and Automation*, pp. 734–739, 1990.

[16] D. Wang and M. Vidyasagar, "Transfer functions foe a single flexible link," *Int. J. of Robotics Research*, vol. 10, no. 5; pp. 540–549, 1991.

[17] A. De Luca and L. Lanari, "Achieving minimum phase behavior in a one-link flexible arm," *1st Int. Symp. on Intelligent Robotics*, pp. 224–235, 1991.

[18] A. De Luca and B. Siciliano, "Regulation of flexible arms under gravity," *IEEE Trans. on Robotics and Automation*, vol. 9, no. 4, pp. 463–467, 1993.

[19] G. Di Giovanni, "Pianificazione e controllo punto-punto di robot con bracci flessibili," Laurea thesis (in Italian), Università di Roma "La Sapienza", March 2001.

[20] A. De Luca and G. Di Giovanni, "Rest-to-rest motion of a two-link robot with a flexible forearm," *2001 IEEE/ASME Int. Conf. on Advanced Intelligent Mechatronics*, July 2001.